Original Research

MNRR1 is a driver of ovarian cancer progression

Hussein Chehade [a],[b], Neeraja Purandare [a], Alexandra Fox [b], Nicholas Adzibolosu [b],
Shawn Jayee [b], Aryan Singh [b], Roslyn Tedja [b], Radhika Gogoi [b], Siddhesh Aras [a],
Lawrence I. Grossman [a], Gil Mor [b], Ayesha B. Alvero [b],[*]

[a] *Center for Molecular Medicine and Genetics, Wayne State University, Detroit, MI, United States*
[b] *C.S. Mott Center for Human Growth and Development, Department of Obstetrics and Gynecology, Wayne State University, Detroit, MI, United States*

ARTICLE INFO

ABSTRACT

Cancer progression requires the acquisition of mechanisms that support proliferative potential and metastatic capacity. MNRR1 (also CHCHD2, PARK22, AAG10) is a bi-organellar protein that in the mitochondria can bind to Bcl-xL to enhance its anti-apoptotic function, or to respiratory chain complex IV (COX IV) to increase mitochondrial respiration. In the nucleus, it can act as a transcription factor and promote the expression of genes involved in mitochondrial biogenesis, migration, and cellular stress response. Given that MNRR1 can regulate both apoptosis and mitochondrial respiration, as well as migration, we hypothesize that it can modulate metastatic spread. Using ovarian cancer models, we show heterogeneous protein expression levels of MNRR1 across samples tested and cell-dependent control of its stability and binding partners. In addition to its anti-apoptotic and bioenergetic functions, MNRR1 is both necessary and sufficient for a focal adhesion and ECM repertoire that can support spheroid formation. Its ectopic expression is sufficient to induce the adhesive glycoprotein *THBS4* and the type 1 collagen, *COL1A1*. Conversely, its deletion leads to significant downregulation of these genes. Furthermore, loss of MNRR1 leads to delay in tumor growth, curtailed carcinomatosis, and improved survival in a syngeneic ovarian cancer mouse model. These results suggest targeting MNRR1 may improve survival in ovarian cancer patients.

Introduction

Cancer initiation and progression involves a series of cellular changes leading to the acquisition of processes that promote enhanced proliferative potential and metastatic capacity. These involve modifications associated with control of growth and cell cycle, focal adhesion, cytoskeleton remodeling, and mitochondrial metabolism [1]. The relevant drivers, which are essential for the continuation of reprogramming towards an aggressive cancer phenotype, have not been clearly defined yet are crucial components for the development of preventative and therapeutic modalities.

Mitochondrial nuclear retrograde regulator 1 (MNRR1; also known as CHCHD2, PARK22, AAG10) is primarily a mitochondrial protein that, depending on its phosphorylation status, binds either the anti-apoptotic protein Bcl-xL [2] or the respiratory chain complex IV (COX IV) [3–5]. Binding to Bcl-xL prevents BAX from forming pro-apoptotic BAX homodimers [2]. On the other hand, phosphorylation at tyrosine 99 (Y99) by ABL2 kinase promotes binding to COX IV, leading to enhanced

respiratory capacity [6]. Additionally, under hypoxic conditions, more specifically at 4% O_2, MNRR1 accumulates in the nucleus, binds to oxygen responsive elements (ORE) on promoter DNA, and transcribes itself as well as other genes related to mitochondrial biogenesis, regulation of ROS, and enhanced mitochondrial respiration [7]. Thus, MNRR1 affects several distinct processes, each of which can independently support an aggressive cancer phenotype and may therefore be a relevant and targetable driver. Indeed, it is overexpressed in multiple cancer types when compared to normal counterparts [4].

Ovarian cancer is a solid tumor with a unique mode of metastasis formation. Unlike breast and prostate cancers, for instance, which preferentially metastasize via the hematogenous route, ovarian cancer cells typically exhibit trans-coelomic metastasis and mostly remain in the peritoneal cavity [8,9]. Although the process of epithelial-mesenchymal transition (EMT) has been implicated in ovarian cancer metastasis, with the loss of E-cadherin and subsequent mesenchymal reprogramming being known to enhance detachment from the primary site and support establishment on secondary sites [10,11], there

are no clinically targetable drivers to date proven to limit ovarian cancer metastasis formation.

In ovarian cancer, the process of metastasis has been divided into 3 sequential steps: detachment from primary tumor, transit, and attachment/colonization of secondary sites [8,12,13]. In the first step, ovarian cancer cells can detach passively from the primary tumor by sloughing off as a result of mechanical forces from the peritoneal fluid, or actively, by initiating an EMT program [14,15]. Either way, for a successful metastasis formation to occur, the detached cells must be able to resist anoikis and inhibit the apoptotic cascade triggered upon detachment. Detached cells can travel to secondary sites either as single cells or as multicellular aggregates or spheroids. In ovarian cancer, spheroid formation has been shown to be critical in the successful dissemination of metastatic cells as detached single cells mostly die upon separation from primary tumor [16,17]. Further, metastasis formation can be greatly enhanced if cells concurrently acquire metabolic flexibility and are able to survive the limited oxygen and nutrient supply during transit to the secondary site. Given that MNRR1 can regulate both apoptosis and mitochondrial respiration [2,5-7], we hypothesize that it is a driver that can be targeted to curtail the metastatic spread of ovarian cancer and delay its progression.

In this study we demonstrate that MNRR1 is expressed and differentially regulated in ovarian cancer cells. In addition to promoting chemoresistance and mitochondrial respiration, as previously described [2,3,6], MNRR1 is required for a focal adhesion and ECM repertoire that can support spheroid formation and promote cytoskeletal remodeling. The loss of this function is sufficient to delay tumor growth, curtail carcinomatosis, and improve survival in a syngeneic ovarian cancer mouse model.

Results

MNRR1 is heterogeneously expressed and regulated in ovarian cancer

We first characterized the expression of MNRR1 in ovarian cancer using human cell lines, primary cell cultures, and whole tumor lysates from ovarian cancer patients. We observed that MNRR1 is expressed in all the cell lines tested with OVCA432 showing the highest expression (Fig. 1A). MNRR1 is also expressed in all the primary cultures tested (PC6, PC8 and PC10) and in whole tumor lysates (T1-T4; Fig. 1B).

Further characterization of the cell lines showed that difference in mRNA levels cannot fully explain the difference in protein expression. OVCA432 for instance showed higher levels of MNRR1 protein than R182 (Fig. 1A) but relative expression of MNRR1 mRNA was higher in R182 compared to OVCA432 (Supplementary Table 1). This suggests that the observed difference in protein expression is due to either post-transcriptional or post-translational regulation. To determine if this mechanism is via regulation of protein stability, we treated R182 and OVCA432 (low and high MNRR1 expression, respectively) with the protein synthesis inhibitor cycloheximide. In R182 we observed that >80% of the MNRR1 protein pool is degraded within 1 hour (Fig. 1C, top panel and 1D). In contrast, in OVCA423, we observed stable levels of MNRR1 even in the presence of cycloheximide (Fig. 1C, bottom panel and 1D). Taken together these results show that MNRR1 is readily translated in ovarian cancer cells and that the heterogeneous protein level observed is in part regulated at the post-translational level.

MNRR1 expression in ovarian cancer cells correlates with mitochondrial function and metabolic flexibility

We then sought to determine whether the expression of MNRR1 correlates with mitochondrial function. To do so, we utilized the MNRR1^low expressing cell line, R182, and the MNRR1^high expressing cell line, OCSC1-F2 (Supp. Fig. 1A). As reported in our previous publications, the MNRR1^low R182 human ovarian cancer cell line is anoikis sensitive and non-tumorigenic [18]. In contrast, the MNRR1^high OCSC1-F2 human ovarian cancer cell line is anoikis resistant and highly tumorigenic [19–24]. We performed the Mito Stress Assay, which measures the cells' oxygen consumption rate (OCR) under basal conditions and in the presence of mitochondrial stressors to inform basal
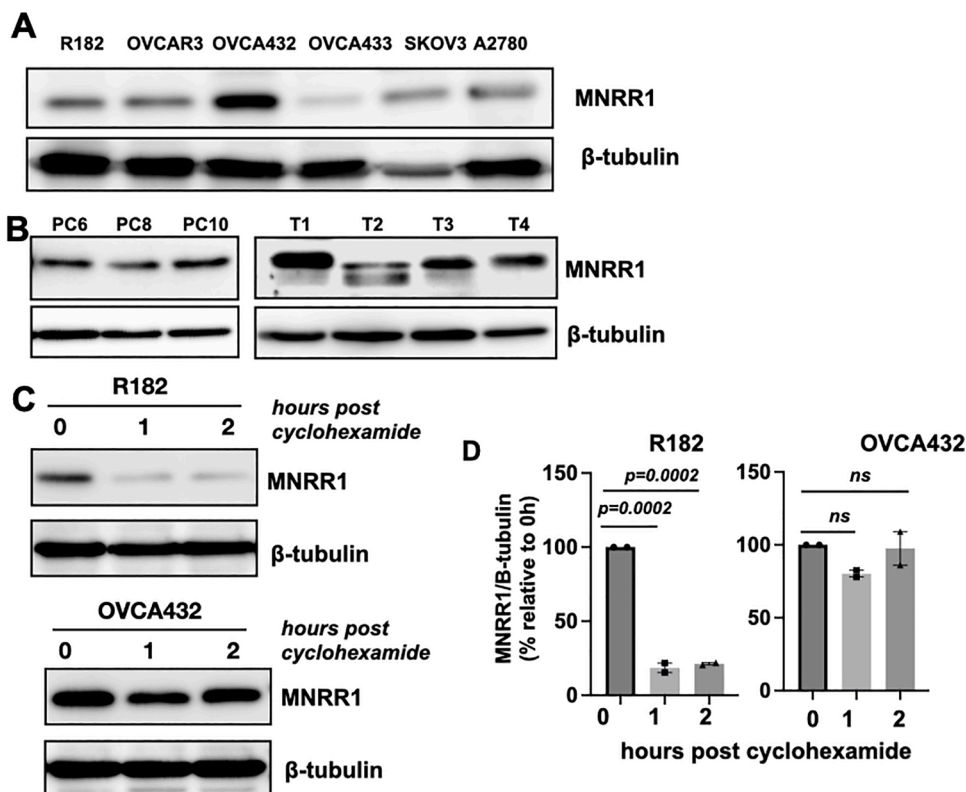
Fig. 1. MNRR1 is expressed in ovarian cancer samples and is regulated post-translationally. Western blot analysis for MNRR1 in (A) human ovarian cancer cell lines; (B) primary cultures (PC) of ovarian cancer cells isolated from ascites or tumors and protein lysates from ovarian tumors (T); (C) R182 (top panel) and OVCA432 (bottom panel) human ovarian cancer cell lines were treated with cycloheximide (20 μg/ml) at designated time-points and levels of MNRR1 were detected by Western blot; (D) quantitation of MNRR1 expression normalized to β-tubulin from C. Values are displayed relative to initial time. Data are presented as mean ± SEM and Ordinary one-way ANOVA with Dunnett's multiple comparison test was used to calculate statistical significance. Experiment was performed twice for each cell line.

mitochondrial respiration, oxygen consumption linked to ATP generation (ATP-linked respiration), and ability to respond to mitochondrial stress or energy demand (spare respiratory capacity). The MNRR1^{high} OCS1-F2 ovarian cancer cell line demonstrated significantly higher mitochondrial function across all parameters tested. Compared to the MNRR1^{low} R182 cell line, OCSC1-F2 cells showed higher basal respiration ($p = 0.0007$), higher ATP-linked respiration ($p = 0.0005$), and higher spare respiratory capacity ($p = 0.0009$) (Supp. Fig. 1B).

We then tested the effect of glucose or glutamine deprivation on cell viability by culturing R182 and OCS1-F2 cells in nutrient-depleted media (as defined in Materials and Methods) supplemented with either glucose or glutamine. Supplementation with glucose allows cells to generate ATP from both the mitochondria and lactic acid route while supplementation with glutamine only supports ATP generation from mitochondria. In the MNRR1^{low} R182 cells, the loss of viability in nutrient depleted media was rescued only with glucose but not with glutamine (Supp. Fig. 1C, left panel). In contrast, in the MNRR1^{high} F2 cells, viability was rescued by either glucose or glutamine (Supp. Fig. 1C, right panel). These results show the correlation between MNRR1 expression, enhanced mitochondrial function and metabolic flexibility.

MNRR1 is sufficient to enhance mitochondrial function and confers metabolic flexibility

So far, our results show correlation between MNRR1 expression and mitochondrial function. To further define its properties, we performed ectopic over-expression. For this, we utilized the MNRR1^{low} R182 human ovarian cancer cell line (Fig. 2A) and performed the Mito Stress

Assay comparing parental R182 cell line with R182 over-expressing MNRR1 (R182 R1 OE) (Fig. 2B). We observed a significant increase in basal respiration) as well as significant increase in ATP-linked respiration and spare respiratory capacity in R182 R1 OE cells compared to the R182 parental cell line. These results demonstrate that MNRR1 is sufficient to enhance mitochondrial respiration in ovarian cancer cells.

To determine if MNRR1 is sufficient to confer metabolic flexibility we used the R182 cell line that is highly dependent on glucose for survival [24]. Thus, we determined cell viability of R182 parental cell line and R182 R1 OE under the different nutrient deprivation states described above. As expected, both R182 parental cell line and R182 R1 OE cells lost viability in the combined absence of glucose and glutamine (Fig. 2C, left panel and 2D). The addition of glucose was sufficient to rescue viability in the R182 parental cell line as we previously reported [24] and also in the R182 R1 OE cells (Fig. 2C, middle panel and 2D). However, the addition of glutamine was not able to rescue cell death in the R182 parental cells, whereas it was able to do so in R182 R1 OE cells (Fig. 2C, right panel and 2D). These results demonstrate that the acquisition of MNRR1 confers metabolic flexibility by allowing cells to utilize glutamine.

MNRR1 is both necessary and sufficient for spheroid formation

To further characterize the role of MNRR1 in ovarian cancer we proceeded to knock-out MNRR1. For this, we utilized the mCherry-expressing TKO mouse ovarian cancer cell line, which is derived from spontaneously formed high-grade serous OC (HGSOC) tumors in a conditional Dicer-PTEN KO mouse with a p53 mutation ($p53$[LSL-R172H/
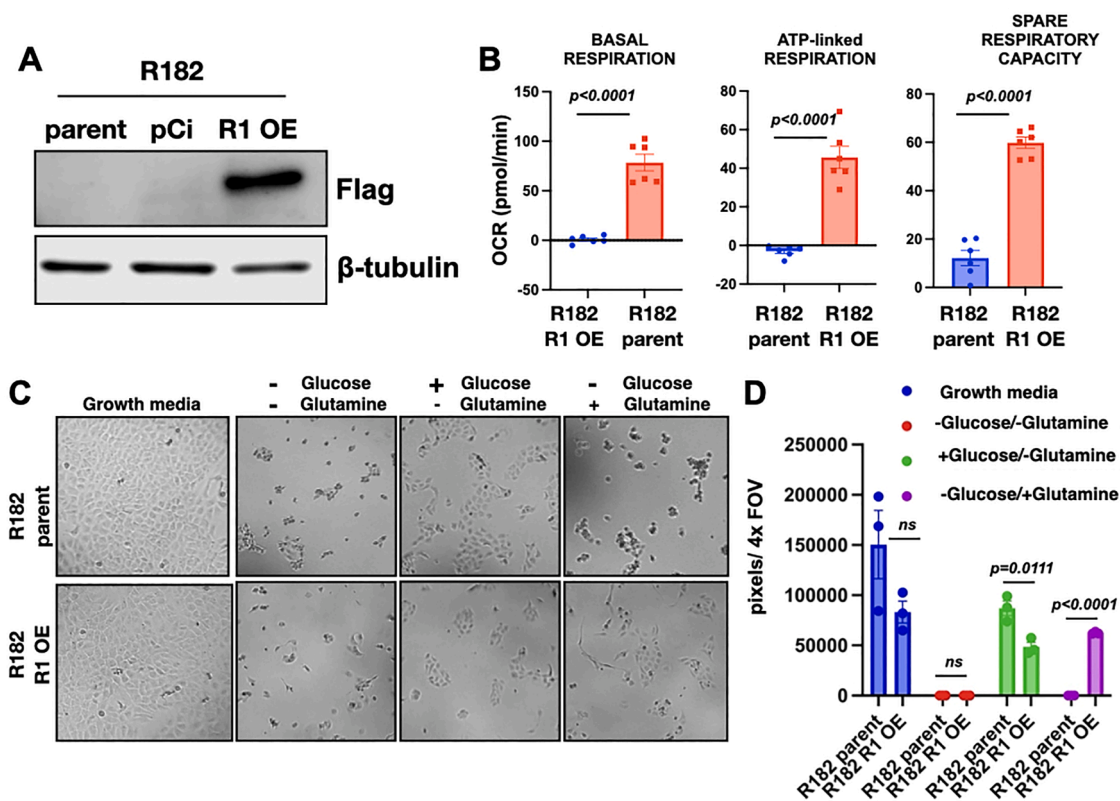
Fig. 2. Ectopic over-expression of MNRR1 enhances mitochondrial respiration in ovarian cancer cells. Flag-tagged MNRR1 was stably over-expressed in the R182 human ovarian cancer cell line. (A) FLAG was detected by Western blot and β-tubulin was used as loading control; (B) Calculated basal respiration, ATP-linked respiration and spare respiratory capacity from Mito Stress Assay. Mito Stress Assay was performed two times and in each experiment, each cell line was ran in triplicate. All datapoints are shown; (C,D) R182 parent and R182 R1 OE cells were cultured under nutrient deprived conditions as detailed in Materials and Methods, supplemented with either glucose (5.5 mM) or glutamine (2 mM), and the effect on cell viability monitored by microscopy and quantified with Image J. Data shown are for 48 h. Data are presented as mean ± SEM and an unpaired *t*-test was used to calculate statistical significance. Three independent experiments were performed and each cell line and culture condition were ran in triplicates. Results shown are for a representative experiment.

$^{+}Dicer^{flox/flox}Pten^{flox/flox}Amhr2^{cre/+})^{25}$. As we previously reported, these cells are anoikis resistant, highly tumorigenic and intra-peritoneal injection in immunocompetent mice results in ascites formation and carcinomatosis within 40 to 50 days [25]. We used CRISPR-Cas9 and successfully knocked-out MNRR1 in these cells (TKO R1 KO) (Fig. 3A). We then assessed mitochondrial respiration comparing TKO R1 KO cells and the TKO parental cell line. Surprisingly, we did not observe a significant change in basal respiration, ATP-linked respiration, or spare respiratory capacity (Supp. Fig. 2A). We also did not observe any changes in substrate utilization when we performed the Mito Fuel Flex Assay (Supp. Fig. 2B). These findings suggest that MNRR1 function is cell-specific. To further examine these observations, we characterized the basal status of MNRR1 in the TKO parental cell line. As mentioned above, in the mitochondria, MNRR1 can bind either COX IV, to improve mitochondrial respiration, or Bcl-xL, to strengthen its anti-apoptotic function [2,6]. We posit that the reason MNRR1 KO did not lead to decreased mitochondrial respiration in TKO cells is that MNRR1 may be mostly bound to Bcl-xL. Indeed, immunoprecipitation (IP) of Bcl-xL and subsequent immunoblotting for MNRR1 showed that in TKO cells, MNRR1 is bound to Bcl-xL (Supp. Fig. 3A). In contrast, when COX IV was immunoprecipitated, we did not observe the presence of MNRR1 in the immunocomplex (Supp. Fig. 3B).

We considered that the MNRR1- Bcl-xL interaction could be associated with the regulation of the apoptotic response. To test this hypothesis, we compared the response of TKO parental cell line and TKO R1 KO to Cisplatin. Our results show that KO of MNRR1 rendered these cells to be more sensitive to Cisplatin as demonstrated by the shift of the IC_{50} for Cisplatin (TKO parent $IC_{50} = 1.8 \mu m$; TKO R1 KO $IC_{50} = 0.004 \mu m$; Supp. Fig. 3C, D).

Anoikis resistance is another critical process wherein the regulation of pro- and anti-apoptotic signals determine cell survival. Given the observed interaction between MNRR1 and Bcl-xL, we tested whether MNRR1 could also facilitate anoikis resistance. Thus, we used the TKO parental cell line and TKO R1 KO cells. The TKO parental cell line is anoikis resistant and forms aggregated spheroids when cultured in ULA

conditions (Fig. 3B, left panel). In contrast, TKO R1 KO cells lost the capacity to form spheroids (Fig. 3B, middle panel) but interestingly, remained viable as quantified in Figure 3Cii. The effect of CRISPR-Cas9-induced MNRR1 loss on spheroid formation was rescued upon re-expression of MNRR1 (Fig. 3B, right panel). Quantification of TKO spheroids are shown in Fig. 3Ci.

We also utilized the R182 parental cell line and R182 R1 OE cells described above. As we previously reported, the R182 parental cell line is anoikis sensitive and non-tumorigenic and culturing these cells in ultra-low attachment (ULA) conditions resulted in activation of apoptosis (Fig. 3D and [18]). In contrast, the R182 R1 OE cells were able to survive ULA and demonstrated an aggregated phenotype (Fig. 3D). Quantification of R182 spheroids are shown in Fig. D, right panel.

MNRR1 reprograms focal adhesion and extra-cellular matrix

To further interrogate the effect of MNRR1 loss in the tumorigenic TKO mouse ovarian cancer cell line, we performed RNA sequencing (GSE218364) followed by Gene Ontology and Pathway Enrichment Analyses comparing TKO R1 KO cells and the TKO parental cell line. Loss of MNRR1 had a major impact on gene expression in these cells. Of the 14,759 measured genes, we observed 3691 differentially expressed genes (DEGs) ($p<0.05$; fold-change (FC) > 0.6). Of these DEGs, 1675 are down-regulated and 2016 genes are up-regulated more than 0.6-fold (Fig. 4A). Supplementary Table 2 lists the top 10 down-regulated and up-regulated genes. Gene Ontology Enrichment Analysis showed 129 Biological Processes that are differentially regulated (FDR<0.05) and the top 25 are shown in Fig. 4B. Pathway Enrichment Analysis showed 24 differentially regulated Pathways (Fig. 4C and Supplementary Table 3). Interestingly, 11 out of the top 25 Biological Processes (marked with * in Fig. 4B) and 2 of the differentially regulated Pathways are associated with cellular locomotion. Network analysis of the DEGs in these locomotion-associated processes showed 10 common genes (Fig. 4D,E), which are mostly associated with focal adhesion and extra-cellular matrix (ECM). *Thbs4*, the most differentially expressed of these
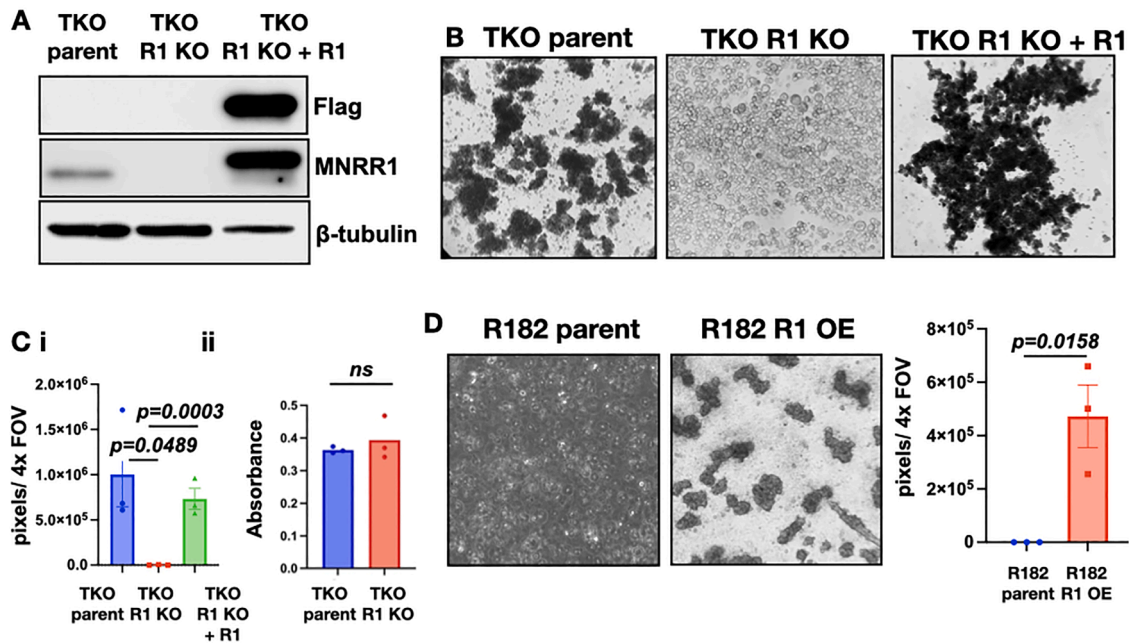
Fig. 3. MNRR1 regulates spheroid formation (A) MNRR1 was deleted (KO) in TKO mouse ovarian cancer cells using CRISPR Cas/9 and rescue experiments were performed by transient overexpression; (B) Cells were cultured on an ultra-low attachment plate; (C) i, spheroids were quantified using Image J; and ii, the effect on cell viability was quantified using Celltiter 96 Aqueous assay; (D) R182 parent and R182 R1 OE cells were cultured on ultra-low attachment plates and effect on spheroid formation was determined by microscopy and quantified using Image J. Data are presented as mean ± SEM and an unpaired *t*-test was used to calculate statistical significance. Three independent experiments were performed and each cell line and culture condition were ran in triplicates. Results shown are for a representative experiment.
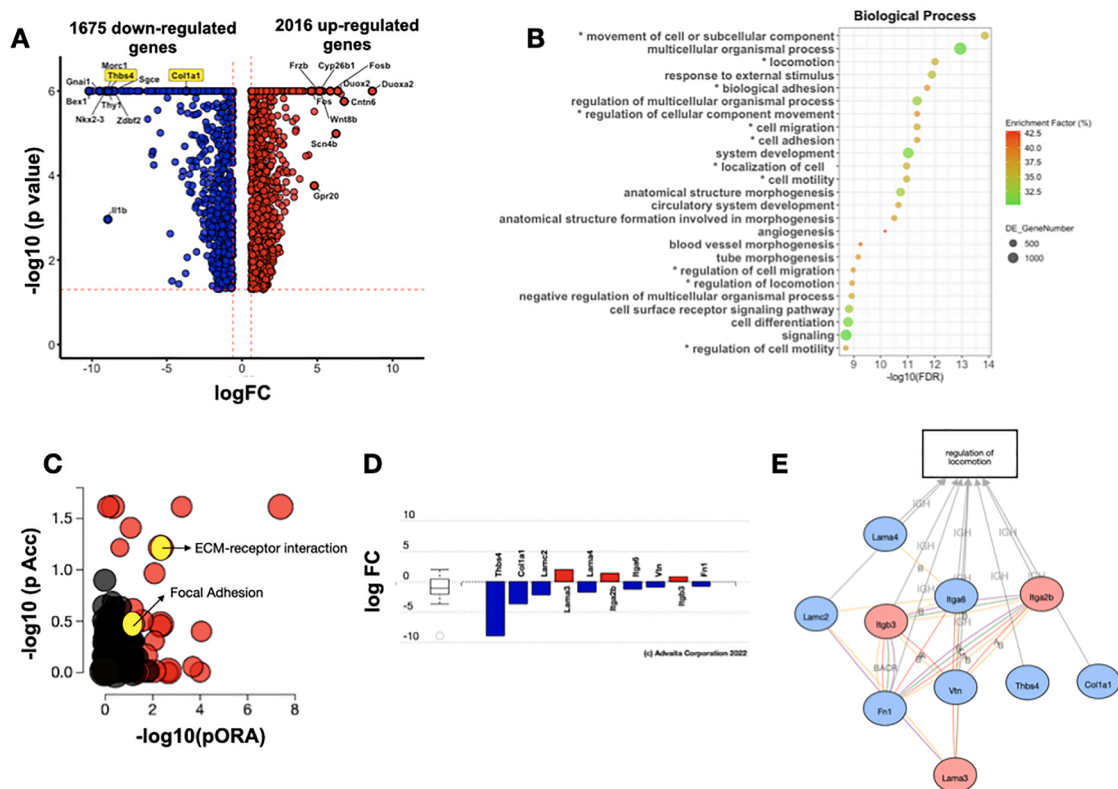
Fig. 4. Effect of MNRR1 on transcriptome. MNRR1 was KO in TKO mouse ovarian cancer cells using CRISPR Cas/9 and the effect on the transcriptome was determined by RNA sequencing. A) Volcano plot of differentially expressed genes (DEGs; (p<0.05; fold-change (FC) > 0.6); location of *Thbs4* and *Col1A1* are shown*;* (B) Differentially regulated Biological Processes in TKO R1 KO cells compared to TKO parental line. *, indicates those related to cell locomotion; (C) Differentially regulated pathways showing both over-representation of DEGs (pORA) and perturbation of the pathway (pAcc); red dots represent significantly different pathways and are listed in Supplementary Table 3; locations of ECM-receptor interaction and focal adhesion are shown; (D) Network analysis of differentially regulated Biological processes and Pathways related to cellular locomotion showed 10 common genes; (E) Subnetwork analysis and interactions of genes in D.

genes ($p = 1 \times 10^{-6}$; FC=−8.97) encodes a protein belonging to the thrombospondin family, which are adhesive glycoproteins that mediate cell-to-cell or cell-to-matrix interactions [26]. *Col1a1*, the second most differentially expressed gene ($p = 1 \times 10^{-6}$; FC=−3.7), encodes type 1 collagen, which is known to promote ovarian cancer metastasis [27]. qPCR (Fig. 5A) and western blot analysis (Fig. 5B) validated the RNA sequencing data and confirmed that Collagen 1A1 is indeed significantly down-regulated in TKO R1 KO cells compared to the TKO parental cell line and, more importantly, rescued upon the ectopic overexpression of MNRR1 (Fig. 5A).

Changes in focal adhesion and ECM are typically transmitted to the cytoskeleton. The filamentous actin (F- actin) cytoskeleton drives the behavior of migrating cells and connects focal adhesion to ECM. Immunofluorescence for F-actin showed intense staining with evident filaments in TKO parent cells (Fig. 5C, left panel). Less intense staining was observed in TKO R1 KO cells (Fig. 5C, right panel).

The effect on focal adhesion, ECM and cytoskeleton arrangement was also observed when MNRR1 was ectopically expressed in the R182 cell line. THBS4 and COL1A1 were significantly up-regulated in R182 R1 OE cells compared to the R182 parental cell line (Fig. 5D and 5E). In addition, immunofluorescence for F-actin showed increase staining in R182 R1 OE cells compared to the R182 parental cell line (Fig. 5F).

Taken together, these results demonstrate that MNRR1 plays an active role in regulating the focal adhesion and ECM repertoire as well as cytoskeleton arrangement in ovarian cancer cells.

Loss of MNRR1 function improves survival in an ovarian cancer mouse model

These cellular results prompted us to determine whether the loss of MNRR1 impacts ovarian cancer progression *in vivo*. Therefore, we compared the growth kinetics of TKO R1 KO and parental TKO cells grown i.p. in immune-competent mice. Live animal imaging (Fig. 6A) and quantification of mCherry signal (Fig. 6B) showed significantly decreased tumor growth in mice injected with TKO R1 KO cells ($p =$ 0.0125 by day 40). Ascites formation was similarly delayed in mice bearing TKO R1 KO cells (Fig. 6C; $p = 0.04$ by 38 days). In addition, survival analysis showed that mice bearing TKO R1 KO cells survived significantly longer (Fig. 6D; $p = 0.0385$) compared to mice bearing parental TKO cells. These results demonstrate that loss of MNRR1 function can curtail ovarian cancer progression and improve survival.

Discussion

We demonstrate here that MNRR1 is heterogeneously expressed and regulated in ovarian cancer cells. Its increased expression is sufficient to improve mitochondrial respiration, confer metabolic flexibility, and promote spheroid formation. In addition, MNRR1 is also required for spheroid formation and loss of this function is adequate to delay tumor growth, the development of carcinomatosis, and improve survival in a syngeneic ovarian cancer mouse model. These results demonstrate that MNRR1 is a relevant driver of ovarian cancer progression (Supp. Fig. 4).

The protein pool of MNRR1 in ovarian cancer cells is tightly controlled at the level of protein stability, wherein in some cells it is rapidly degraded within 1 hour of its translation. Although it may seem
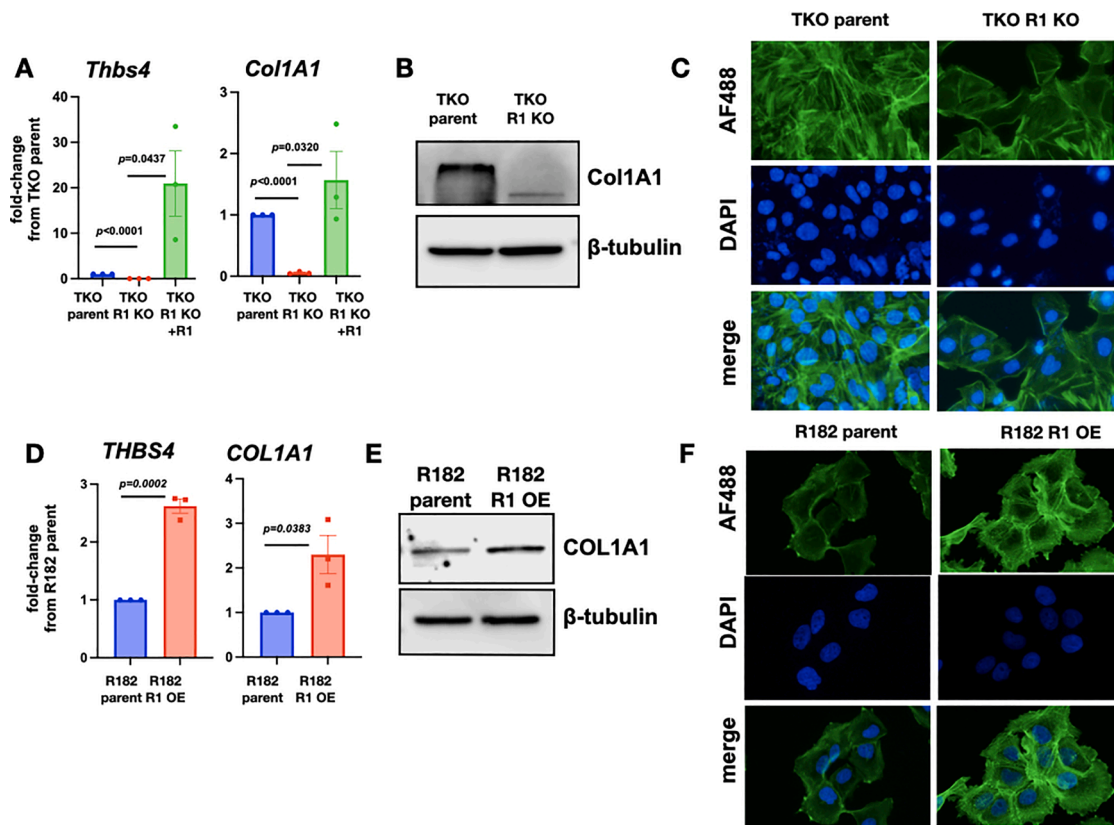
Fig. 5. MNRR1 reprograms focal adhesion and extra-cellular matrix. MNRR1 was KO in TKO mouse ovarian cancer cells using CRISPR Cas/9. (A) mRNA levels of *Thbs4* and *Col1A1* were quantified by qPCR in TKO parent, TKO R1 KO, and TKO R1 KO with overexpressed MNRR1 (TKO R1 KO + R1). Data are presented as mean ± SEM and unpaired *t*-test was used to calculate statistical significance; (B) Protein levels of Col1A1 were determined by western blot analysis; (C) Level and distribution of F-actin were determined by immunofluorescence as described in the Materials and Methods section; (D) MNRR1 was overexpressed in R182 cell line and mRNA levels of *THBS4* and *COL1A1* were quantified by qPCR. Data are presented as mean ± SEM and an unpaired *t*-test was used to calculate statistical significance; (E) Protein levels of COL1A1 were determined by western blot analysis; (F) Level and distribution of F-actin were determined by immunofluoresence.

counterintuitive to devote cellular energy to translating a protein and then rapidly targeting it for degradation, this mode of regulation can allow for a prompter response to external stimuli. Given that MNRR1 can confer several pro-tumor functions such as inhibition of apoptosis and improved mitochondrial respiration [2,6], mechanisms permitting its rapid upregulation will confer advantages for cancer cell survival and support metastatic spread. Stimuli in the ovarian tumor microenvironment that can upregulate MNRR1 are currently being investigated in our lab. We previously showed that the protease, YME1L1, is a major effector of MNRR1 degradation [28] and we detected YME1L1 in all of the ovarian cancer samples tested but did not find any correlation between YME1L1 and MNRR1 levels (data not shown). It is possible that another layer of regulation is in place that can dictate the action of YME1L1 on MNRR1 in ovarian cancer cells.

In addition to variability in levels, we also observed differential regulation and functionality of MNRR1 in ovarian cancer cells. When over-expressed in the R182 cells, MNRR1 enhanced mitochondrial respiration and acquisition of metabolic flexibility. In the tumorigenic TKO mouse ovarian cancer cell line, basal MNRR1 is mostly bound to Bcl-xL rather than to the electron transport chain. It was therefore not surprising to observe that KO of MNRR1 in TKO cells did not lead to decreased mitochondrial respiration or less metabolic flexibility but instead lead to greater sensitivity to Cisplatin. Consistently, loss of MNRR1 in these cells affected focal adhesion and ECM proteins.

Since the TKO parental cells are tumorigenic, does the observation that these cells do not have enhanced spare respiratory capacity suggest that enhanced mitochondrial respiration is not required for tumorigenicity per se? Since it is possible that i.p. injection of TKO R1 KO cells in mice can result in cellular adaptation that may affect MNRR1-

independent increase in mitochondrial function, the answer to this question is not well-defined. Nevertheless, it is clear that loss of MNRR1 is sufficient to curtail ovarian cancer progression and improve survival.

The change in focal adhesion and ECM repertoire as well as cyto-skeleton re-organization observed in the TKO R1 KO cells may very well be the underlying mechanism for the detected delay in disease progression. As stated above, ovarian cancer cells can passively or actively detach from the primary tumor and can remain in the peritoneal cavity as single cell suspension or aggregate and form spheroids. The formation of spheroids has been shown to support pro-tumor functions by improving survival, enhancing invasive potential, conferring chemo-resistance and improving immune escape [16,29–31]. TKO R1 KO cells were still able to form tumors although tumor growth was delayed. Given that the TKO R1 KO cells maintained anoikis resistance but lost the ability to form aggregated spheroids, our results suggest that anoikis resistance may be more essential during tumor formation but cell aggregation may contribute more to disease progression. Several focal adhesion and ECM proteins were also downregulated when MNRR1 was deleted in HEK-293 cells and rescued upon re-expression of transcriptionally active MNRR14. Similar to what was observed in the TKO cell line, the changes were primarily at the mRNA level. Given that MNRR1's transcriptional activity is enhanced at low oxygen levels, it is thus interesting to observe these transcriptional effects on focal adhesion and ECM genes in the TKO cell line grown under typical culture conditions. It should also be noted that the altered effect on spheroid formation is the common outcome of MNRR1 overexpression in human R182 ovarian cancer cells and MNRR1 KO in mouse TKO ovarian cancer cells.

The observed effect of MNRR1 loss in ovarian cancer progression demonstrates that it is a relevant target, which might improve survival
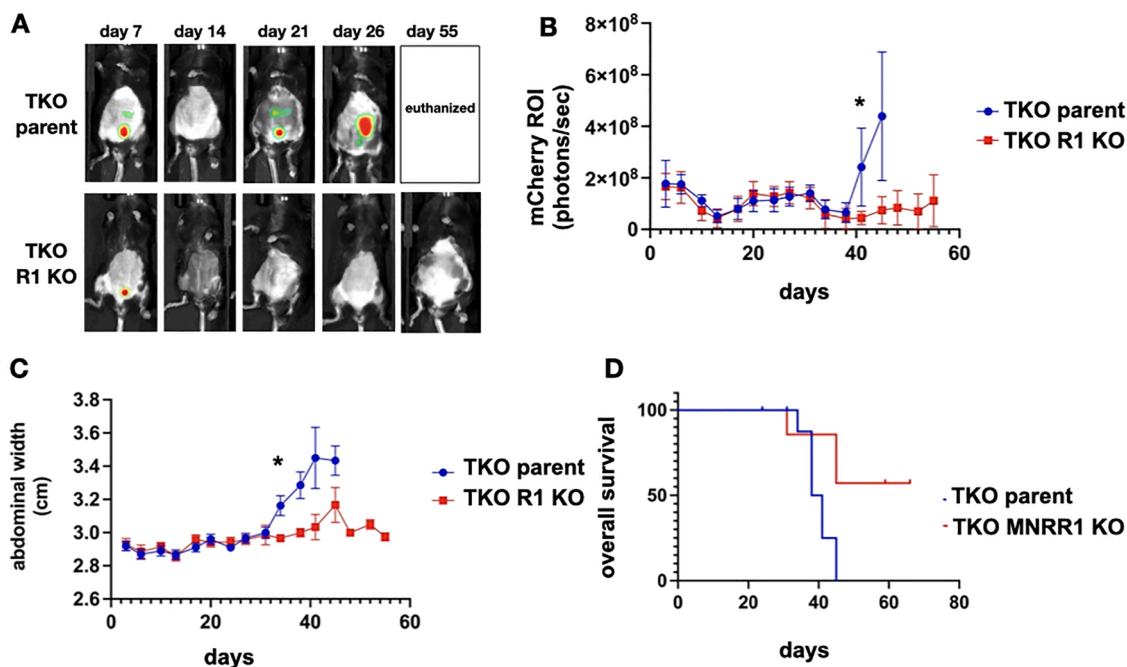
Fig. 6. Loss of MNRR1 improves overall survival in a syngeneic mouse model of ovarian cancer. 1×10^7 mCherry+ TKO parent ($n = 10$) or mCherry+ TKO R1 KO cells were injected i.p. in C57/BL6 immunocompetent mice ($n = 7$). (A) Fluorescence imaging of TKO parent and TKO R1 KO cells injected i.p. in C57BL6 mice; (B) mCherry signal from region of interest (ROI) was quantified to graph tumor growth, * $p = 0.0125$; (C) Ascites formation was determined by measuring abdominal width, * $p = 0.0402$; (D) Overall survival defined as the day abdominal width >3.4 cm, * $p = 0.0385$. Data are presented as mean ± SEM and one-way ANOVA was used to calculate statistical significance.

in ovarian cancer patients. We previously reported that a pharmacological inhibitor of MNRR1, Clotrimazole, is able to inhibit MNRR1 expression in human trophoblast cells [32]. Further studies are required to determine the *in vivo* activity and selectivity of Clotrimazole against MNRR1. Nevertheless, our results clearly demonstrate that successful inhibition of MNRR1 can significantly delay ovarian cancer progression.

In conclusion, we demonstrate that MNRR1 is tightly regulated post-translationally. Its multi-modal regulation at the levels of protein stability, cellular location and protein-protein binding allows it to promptly confer its pro-survival benefits. This is especially helpful in the context of ovarian cancer dissemination, which to be successful, requires cells to rapidly adapt to the changing constraints of its microenvironment. This mode of regulation precludes MNRR1 from being a biomarker for patient survival. However, the demonstration that its loss can significantly delay disease progression suggest that MNRR1 can be a valuable clinical target in ovarian cancer.

Materials and methods

Cell lines and culture conditions

Human ovarian cancer cell lines OVCA432 (RRID:CVCL_3769), OVCAR3 (RRID:CVCL_DH37), OVCA433 (RRID:CVCL_0475), and CaOV3 (RRID:CVCL_0475) were obtained from ATCC. Human ovarian cancer cell lines R182, R2615 and OCSC1-F2 were isolated from tumors derived from ovarian cancer patients as previously described[19,21-24, 33,34]. These cell lines were cultured in RPMI media supplemented with 10% FBS, 1% Penicillin-Streptomycin, 1% Sodium Pyruvate, 1% HEPES, and 1% non-essential amino acids. The TKO mouse ovarian cancer cell line (gift from Dr. Martin Matzuk)[35] was cultured in DMEM/F12 media supplemented with 10% FBS and 1% Penicillin-Streptomycin. Cells were grown at 37 °C with 5% CO_2. All cell lines were routinely tested for mycoplasma and authenticated once a year by STR profiling and used within 6 passages between experiments.

For nutrient deprivation assay, cells were cultured in SILAC RPMI

1640 Flex media (Thermo Scientific, Waltham, MA) supplemented with either 5.5 mM Glucose (Fisher Scientific, Pittsburgh, PA) or 2 mM Glutamax (Thermo Scientific). For the anoikis assay, cells were cultured in ultra-low attachment plates (Corning, Corning, NY). Microscopy was used to determine effect on cells. Live cells and spheroids were quantified using ImageJ (RRID:SCR_003070).

Human subjects

The use of all human samples was approved by Wayne State University IRB (IRB-20–07–2521) and Karmanos Cancer Institute IRB (IRB 2013–052). The three fresh ovarian tumors used in the establishment of primary cell cultures (PC6, PC8 and PC10) were consecutively collected during debulking surgery from patients diagnosed with high-grade serous ovarian cancer irrespective of patient age, tumor grade, tumor stage or previous treatment and de-identified by the Biobanking and Correlative Sciences Core at Wayne State University and Karmanos Cancer Institute. Tumors were minced and 0.1 g of tissue was dissociated with 0.1% collagenase at 37oC for 30 mins. Dissociated tissue was passed though 100 um filter mesh and washed with PBS. After RBC lysis, cells were grown in Media 199/105 supplemented with 15% FBS, 1% Penicillin-Streptomycin, 1% Sodium Pyruvate, 1% HEPES, and 1% non-essential amino acids. Protein lysates were collected from monolayer cells between passage 4 to 6.

The four frozen ovarian tumors used (T1, T2, T3 and T4) were requested from Biobanking and Correlative Sciences Core at Wayne State University and Karmanos Cancer Institute. Protein lysates were obtained by tissue homogenization using Zirconium beads and Cell lysis buffer (Cell Signaling Technologies, Danvers, MA).

All patients were diagnosed with high-grade serous ovarian cancer and underwent surgery at Karmanos Cancer Institute. No other selection criteria were used.

Ectopic expression and knock-out of MNRR1

A g-block DNA sequence was obtained (IDT DNA, Coralville, IA, USA) such that when inserted into the multiple cloning site would express human MNRR1. The product was amplified using primers harboring the cloning sites XbaI and XhoI. The primers used also added a 3xFlag epitope at the c-terminus (Supp. Fig. 5). The digested amplified product was ligated into pCI-Neo vector, transformed into DH5alpha competent cells and DNA extracted using a Maxiprep kit (Qiagen, Valencia, CA, USA).

Cells were plated one day prior to transfection in 60 mm dishes at a concentration of 200,000 cells/dish. The following day, 2 µg of MNRR1 plasmid was transfected into cells using Fugene HD (Promega, Madison, WI). 48 hrs after transfection, cells were selected using 2 mg/ml G418 (Invivogen, San Diego, CA).

MNRR1 was knocked-out using CHCHD2 CRISPR/Cas9 KO plasmid (SC-420238; https://datasheets.scbt.com/sc-420238.pdf) purchased from Santa Cruz Biotechnologies (Dallas, TX) and used as previously described [28].

Mito Stress Assay

Cellular oxygen consumption at baseline or in the presence of mitochondrial stressors (Mito Stress Assay) was measured using Seahorse XFe24 Bioanalyzer (Agilent, Santa Clara, CA; RRID:SCR_019539) according to manufacturer's instructions. Cells were plated at a concentration of 35,000 cells/well 24 h prior to the assay.

In vivo tumor formation

All the described experiments using mice were approved by Wayne State University Animal Care and Use Committee (IACUC 22–03–4474) and mice were house at Wayne State University Division of Laboratory Animal Resources. For assessing the tumorigenic potential, 1×10^7 mCherry-expressing TKO parent or TKO R1 KO cells were randomly injected intraperitoneally (i.p.) in C57BL6 mice (Jackson Laboratory, Bar Harbor, ME) ($n = 10$ and $n = 7$, respectively). Mice were imaged twice a week using Ami HT Imaging System (Spectral Instruments, Tucson, AZ) and mCherry fluorescent signal was measured using Aura Imaging Software to quantify tumor burden. Tumor growth was graphed using GraphPad Prism v9.3.1(San Diego, CA; RRID:SCR_002798) and statistical significance calculated using One way ANOVA. Animal weight and abdominal width were monitored twice weekly. Abdominal width was graphed using GraphPad Prism and statistical significance calculated using One way ANOVA. Animals were sacrificed when mCherry signal exceeded 1×10^9 photons/sec or when abdominal width reached 3.4 cm. These values were used to determine overall survival. Survival was graphed and calculated using GraphPad Prism v9.3.1. All mice were included in the analysis. Investigators were aware of group allocation.

Statistical analysis

Unpaired two-tailed Student t-tests assuming Gaussian distribution or one way analysis of variance (ANOVA) with dunnett's multiple comparisons were used for comparison between different groups. *P* values of 0.05 or less were considered statistically significant. Statistical analysis were performed and all data were graphed using GraphPad Prism v9.3.1(San Diego, CA; RRID:SCR_002798). Data are presented as mean ±SEM. Specific analysis are elaborated in each Figure legend.

Additional Methods are described as Supplementary Material.

Data availability statement

The datasets generated during and/or analysed during the current study have been deposited and will be made available upon publication (GSE218364).

CRediT authorship contribution statement

Hussein Chehade: Investigation, Validation, Formal analysis, Writing – original draft. **Neeraja Purandare:** Methodology, Data curation. **Alexandra Fox:** Investigation. **Nicholas Adzibolosu:** Software. **Shawn Jayee:** Investigation. **Aryan Singh:** Investigation. **Roslyn Tedja:** Investigation. **Radhika Gogoi:** Resources. **Siddhesh Aras:** Methodology, Conceptualization, Writing – original draft. **Lawrence I. Grossman:** Conceptualization, Writing – original draft. **Gil Mor:** Conceptualization, Writing – original draft, Funding acquisition. **Ayesha B. Alvero:** Conceptualization, Formal analysis, Visualization, Writing – original draft, Supervision, Project administration.

Declaration of Competing Interest

The authors declare that they have no known competing financial interests or personal relationships that could have appeared to influence the work reported in this paper.

Acknowledgement

Supplementary materials

Supplementary material associated with this article can be found, in the online version, at doi:10.1016/j.tranon.2023.101623.

References

[1] D. Hanahan, R.A. Weinberg, Hallmarks of cancer: the next generation, Cell 144 (5) (2011) 646–674, https://doi.org/10.1016/j.cell.2011.02.013.

[2] Y. Liu, H.V. Clegg, P.L. Leslie, et al., CHCHD2 inhibits apoptosis by interacting with Bcl-x L to regulate Bax activation, Cell Death Differ. 22 (6) (2015) 1035–1046, https://doi.org/10.1038/cdd.2014.194.

[3] L.I. Grossman, N. Purandare, R. Arshad, et al., MNRR1, a biorganellar regulator of mitochondria, Oxid. Med. Cell Longev. 2017 (2017), 6739236, https://doi.org/10.1155/2017/6739236.

[4] S. Aras, M.C. Maroun, Y. Song, et al., Mitochondrial autoimmunity and MNRR1 in breast carcinogenesis, BMC Cancer 19 (1) (2019) 411, https://doi.org/10.1186/s12885-019-5575-7.

[5] S. Aras, M. Bai, I. Lee, R. Springett, M. Huttemann, L.I. Grossman, MNRR1 (formerly CHCHD2) is a bi-organellar regulator of mitochondrial metabolism, Mitochondrion 20 (2015) 43–51, https://doi.org/10.1016/j.mito.2014.10.003.

[6] S. Aras, H. Arrabi, N. Purandare, et al., Abl2 kinase phosphorylates bi-organellar regulator MNRR1 in mitochondria, stimulating respiration, Biochim. Biophys. Acta Mol. Cell Res. 1864 (2) (2017) 440–448, https://doi.org/10.1016/j.bbamcr.2016.11.029.

[7] N. Purandare, M. Somayajulu, M. Huttemann, L.I. Grossman, S. Aras, The cellular stress proteins CHCHD10 and MNRR1 (CHCHD2): partners in mitochondrial and nuclear function and dysfunction, J. Biol. Chem. 293 (17) (2018) 6517–6529, https://doi.org/10.1074/jbc.RA117.001073.

[8] E. Lengyel, Ovarian cancer development and metastasis, Am. J. Pathol. 177 (3) (2010) 1053–1064, https://doi.org/10.2353/ajpath.2010.100105.

[9] S.J. Ritch, C.M. Telleria, The transcoelomic ecosystem and epithelial ovarian cancer dissemination, Front. Endocrinol. 13 (2022), 886533, https://doi.org/10.3389/fendo.2022.886533.

[10] S. Elloul, M.B. Elstrand, J.M. Nesland, et al., Snail, Slug, and Smad-interacting protein 1 as novel parameters of disease aggressiveness in metastatic ovarian and breast carcinoma, Cancer 103 (8) (2005) 1631–1643, https://doi.org/10.1002/cncr.20946.

[11] L.G. Hudson, R. Zeineldin, M.S. Stack, Phenotypic plasticity of neoplastic ovarian epithelium: unique cadherin profiles in tumor progression, Clin. Exp. Metastasis 25 (6) (2008) 643–655, https://doi.org/10.1007/s10585-008-9171-5.

[12] M. AK, Ovarian cancer metastasis: a unique mechanism of dissemination, in: K X (Ed.), Tumor Metastasis, Intech, London, 2016.

[13] H. Chehade, R. Tedja, H. Ramos, et al., Regulatory role of the adipose microenvironment on ovarian cancer progression, Cancers 14 (9) (2022), https://doi.org/10.3390/cancers14092267.

[14] B. Davidson, C.G. Trope, R. Reich, Epithelial-mesenchymal transition in ovarian carcinoma, Front. Oncol. 2 (2012) 33, https://doi.org/10.3389/fonc.2012.00033.

[15] T. Kan, W. Wang, P.P. Ip, et al., Single-cell EMT-related transcriptional analysis revealed intra-cluster heterogeneity of tumor cell clusters in epithelial ovarian

cancer ascites, Oncogene 39 (21) (2020) 4227–4240, https://doi.org/10.1038/s41388-020-1288-2.

[16] S.L.E. Compton, E.S. Pyne, L. Liu, et al., Adaptation of metabolism to multicellular aggregation, hypoxia and obese stromal cell incorporation as potential measure of survival of ovarian metastases, Exp. Cell. Res. 399 (1) (2021), 112397, https://doi.org/10.1016/j.yexcr.2020.112397.

[17] S. Farsinejad, T. Cattabiani, T. Muranen, M. Iwanicki, Ovarian cancer dissemination-a cell biologist's perspective, Cancers 11 (12) (2019), https://doi.org/10.3390/cancers11121957.

[18] J. Li, A.B. Alvero, S. Nuti, et al., CBX7 binds the E-box to inhibit TWIST-1 function and inhibit tumorigenicity and metastatic potential, Oncogene 39 (20) (2020) 3965–3979, https://doi.org/10.1038/s41388-020-1269-5 (In eng).

[19] A.N. van den Pol, X. Zhang, E. Lima, et al., Lassa-VSV chimeric virus targets and destroys human and mouse ovarian cancer by direct oncolytic action and by initiating an anti-tumor response, Virology 555 (2021) 44–55, https://doi.org/10.1016/j.virol.2020.10.009 (In eng).

[20] C. Cardenas, M.K. Montagna, M. Pitruzzello, E. Lima, G. Mor, A.B. Alvero, Adipocyte microenvironment promotes Bcl(xl) expression and confers chemoresistance in ovarian cancer cells, Apoptosis 22 (4) (2017) 558–569, https://doi.org/10.1007/s10495-016-1339-x (In eng).

[21] A.B. Alvero, D. Kim, E. Lima, et al., Novel approach for the detection of intraperitoneal micrometastasis using an ovarian cancer mouse model, Sci. Rep. 7 (2017) 40989, https://doi.org/10.1038/srep40989 (In eng).

[22] A.B. Alvero, A. Heaton, E. Lima, et al., TRX-E-002-1 induces c-jun-dependent apoptosis in ovarian cancer stem cells and prevents recurrence in vivo, Mol. Cancer Ther. 15 (6) (2016) 1279–1290, https://doi.org/10.1158/1535-7163.MCT-16-0005.

[23] N.J. Sumi, E. Lima, J. Pizzonia, et al., Murine model for non-invasive imaging to detect and monitor ovarian cancer recurrence, J. Vis. Exp. (93) (2014) e51815, https://doi.org/10.3791/51815.

[24] A.B. Alvero, M.K. Montagna, N.J. Sumi, W.D. Joo, E. Graham, G. Mor, Multiple blocks in the engagement of oxidative phosphorylation in putative ovarian cancer stem cells: implication for maintenance therapy with glycolysis inhibitors, Oncotarget 5 (18) (2014) 8703–8715, https://doi.org/10.18632/oncotarget.2367.

[25] A.B. Alvero, D. Hanlon, M. Pitruzzello, et al., Transimmunization restores immune surveillance and prevents recurrence in a syngeneic mouse model of ovarian cancer, Oncoimmunology 9 (1) (2020), 1758869, https://doi.org/10.1080/2162402X.2020.1758869.

[26] C. Zhang, C. Hu, K. Su, et al., The integrative analysis of thrombospondin family genes in pan-cancer reveals that THBS2 facilitates gastrointestinal cancer metastasis, J. Oncol. 2021 (2021), 4405491, https://doi.org/10.1155/2021/4405491.

[27] M. Li, J. Wang, C. Wang, et al., Microenvironment remodeled by tumor and stromal cells elevates fibroblast-derived COL1A1 and facilitates ovarian cancer metastasis, Exp. Cell. Res. 394 (1) (2020), 112153, https://doi.org/10.1016/j.yexcr.2020.112153.

[28] S. Aras, N. Purandare, S. Gladyck, et al., Mitochondrial Nuclear Retrograde Regulator 1 (MNRR1) rescues the cellular phenotype of MELAS by inducing homeostatic mechanisms, Proc. Natl. Acad. Sci. USA 117 (50) (2020) 32056–32065, https://doi.org/10.1073/pnas.2005877117.

[29] Y. He, A.C. Wu, B.S. Harrington, et al., Elevated CDCP1 predicts poor patient outcome and mediates ovarian clear cell carcinoma by promoting tumor spheroid formation, cell migration and chemoresistance, Oncogene 35 (4) (2016) 468–478, https://doi.org/10.1038/onc.2015.101.

[30] J. Ogishima, A. Taguchi, A. Kawata, et al., The oncogene KRAS promotes cancer cell dissemination by stabilizing spheroid formation via the MEK pathway, BMC Cancer 18 (1) (2018) 1201, https://doi.org/10.1186/s12885-018-4922-4.

[31] R.A. Davidowitz, L.M. Selfors, M.P. Iwanicki, et al., Mesenchymal gene program-expressing ovarian cancer spheroids exhibit enhanced mesothelial clearance, J. Clin. Invest. 124 (6) (2014) 2611–2625, https://doi.org/10.1172/JCI69815.

[32] Purandare N., Kunji Y., Xi Y., Romero R., Gomez-Lopez N., Fribley A., Grossman L., Aras S. Lipopolysaccharide induces placental mitochondrial dysfunction by reducing MNRR1 levels via a TLR4-independent pathway.

[33] R. Tedja, C.M. Roberts, A.B. Alvero, et al., Protein kinase Cα-mediated phosphorylation of Twist1 at Ser-144 prevents Twist1 ubiquitination and stabilizes it, J. Biol. Chem. 294 (13) (2019) 5082–5093, https://doi.org/10.1074/jbc.RA118.005921 (In eng).

[34] C. Cardenas, M.K. Montagna, M. Pitruzzello, E. Lima, G. Mor, A.B. Alvero, Adipocyte microenvironment promotes Bclxl expression and confers chemoresistance in ovarian cancer cells, Apoptosis 22 (4) (2017) 558–569, https://doi.org/10.1007/s10495-016-1339-x.

[35] J. Kim, D.M. Coffey, L. Ma, M.M. Matzuk, The ovary is an alternative site of origin for high-grade serous ovarian cancer in mice, Endocrinology 156 (6) (2015) 1975–1981, https://doi.org/10.1210/en.2014-1977.